From a Road Less Travelled to a Worn Path: Three-Dimensional Tumour Models for Cancer Research and Therapeutics

Malakpour Permlid, Atena

2020

Document Version:
Peer reviewed version (aka post-print)

Toxicology in Vitro 60 (2019) 51–60

Contents lists available at ScienceDirect

Toxicology in Vitro

journal homepage: www.elsevier.com/locate/toxinvit

Unique animal friendly 3D culturing of human cancer and normal cells

Atena Malakpour Permlid*, Plaurent Roci, Elina Fredlund, Felicia Fält, Emil Önell, Fredrik Johansson, Stina Oredsson

Department of Biology, Lund University, Sölvegatan 35, 223 62 Lund, Sweden

ARTICLE INFO

Keywords:
Electrospinning
3D polycaprolactone meshes
Extracellular matrix
Biocompatibility
Donor horse serum
Tumour microenvironment

ABSTRACT

Two-dimensional cell culturing has proven inadequate as a reliable preclinical tumour model due to many inherent limitations. Hence, novel three-dimensional (3D) cell culture models are needed, which in many aspects can mimic a native tumour with 3D extracellular matrix. Here, we present a 3D electrospun polycaprolactone (PCL) mesh mimicking the collagen network of tissue. The naturally hydrophobic PCL mesh was subjected to O_2 plasma treatment to obtain hydrophilic fibres. Biocompatibility tests performed using L929 fibroblasts show that the 3D PCL fibre unit compartments were non-toxic. The human breast cancer cell lines MCF-7 and JIMT-1, the normal-like human breast cell line MCF-10A, and human adult fibroblast were cultured in PCL meshes and cell proliferation was monitored using the AlamarBlue® assay. Confocal microscopy and cryosectioning show that the cells penetrated deep into the fibre mesh within 1 week of cell culturing. The cancer cells form spheroids with the cells attaching mainly to each other and partly to the fibres. The human adult fibroblasts stretch out along the fibres while the MCF-10A cells stretch between fibres. Overall, we show that normal and cancer cells thrive in the 3D meshes cultured in fetal bovine free medium which eliminates the use of collagen as an extracellular matrix support.

1. Introduction

Preclinical studies to unravel the biology of human cancers and to develop new treatment strategies have traditionally been carried out using conventional two-dimensional (2D) cell cultures. However, these cancer models have proven inadequate as reliable preclinical tumour models due to many inherent limitations (Kim, 2005; Szot et al., 2011). One major drawback of 2D cell culture models is the lack of three-dimensional (3D) microenvironmental cues that exist *in vivo* (Feng et al., 2013). The *in vivo* tissue microenvironment consists of a complex 3D extracellular matrix (ECM) formed mainly by stromal cells (Feng et al., 2013; Kim, 2005; Rijal and Li, 2016). The mechanical, structural, and biochemical cues which support cell-cell and cell-matrix interactions in a 3D microenvironment are mostly absent in 2D models (Feng et al., 2013; Kim, 2005; Szot et al., 2011). Laboratory animal experiments have contributed substantially to our current understanding of human cancer biology and drug sensitivity; however, there are fundamental genetic, metabolic, and ontogenetic differences between tumours in humans and xenografted human tumours (Anisimov et al., 2005; Rangarajan and Weinberg, 2003; Rangarajan et al., 2004). Hence, novel 3D cell culture models are needed, which in many aspects can mimic the native human extracellular matrix with embedded cells. Moreover, cell-based 3D techniques provide an opportunity to use an alternative *in vitro* method in compliance with the replacement of animal experiments in 3R recommendations. In fact, 3D models are increasingly used in cancer research and one commonly used product to obtain a 3D fibrous structure to support cells is matrigel extracted from the Engelbreth-Holm-Swarm (EHS) mouse sarcoma (Nyga et al., 2011; Bielecka et al., 2017). However, in the strive to replace animal experiments, it is advisable to eliminate animal-derived products in cell culturing that are obtained causing animal suffering. Unfortunately, a continuous supply of the EHS mouse sarcoma-derived matrigel requires serial transplantation of mice with the EHS tumour. Thus, in the present work we have used polycaprolactone (PCL) to produce a 3D collagen-mimicking synthetic scaffold. PCL is widely used by researchers because of its low melting point, viscoelastic properties, blend-compatibility, and long-term biodegradability (Cipitria et al., 2011; Wu and Hong, 2016). The Food and Drug Administration has approved PCL for specific applications in the human body such as for drug delivery and suture materials (Ulery et al., 2011).

Abbreviations: 2D, two-dimensional; 3D, three-dimensional; ECM, extracellular matrix; PCL, polycaprolactone; PLA, polylactic acid; TME, tumour microenvironment; FBS, fetal bovine serum; DHS, donor horse serum; SEM, scanning electron microscope

* Corresponding author at: Department of Biology, Lund University, Sölvegatan 35C, 223 62 Lund, Sweden.
E-mail address: atena.malakpour_permlid@biol.lu.se (A. Malakpour Permlid).

https://doi.org/10.1016/j.tiv.2019.04.022
Received 22 August 2018; Received in revised form 18 April 2019; Accepted 18 April 2019
Available online 10 May 2019

Among various techniques for manufacturing of 3D scaffolds, electrospinning is a cost-effective and simple process that allows the formation of polymer fibres with sub-micron diameter resembling the non-woven fibrous collagen structure of the ECM (Cipitria et al., 2011; Frenot and Chronakis, 2003; Martins et al., 2009; Jakobsson et al., 2017). Randomly electrospun fibre meshes create high surface-area-to-volume ratio for cell attachment and provide a natural 3D tissue like structure enabling oxygen and nutrient gradients due to their porosity (Cipitria et al., 2011; Knight and Przyborski, 2015). Studies of breast cancer cell proliferation, adhesion, and survival on electrospun 2D and 3D PCL fibrous scaffolds have been reported (Feng et al., 2013; Foroni et al., 2013; Rijal and Li, 2016). However, a synthetic 3D culture with strong infiltration of cancer cells into the depth of the 3D system still needs to be developed (Kim et al., 2016). Here, we present a fully synthetic and highly porous 3D PCL fibre mesh suspended in a polylactic acid (PLA) ring structure and show that cells can invade into the porous structure of the fibre mesh.

To further comply to the replacement of less defined products derived through animal ethically questionable procedures, we have replaced fetal bovine serum (FBS) with donor horse serum (DHS) in the cell culture medium of the various cell types used in this study. FBS is produced by obtaining blood through heart puncture of live calf foetuses that have been extracted from the womb of pregnant cows at slaughter (van der Valk et al., 2004). Collection of blood from donor horses of donor herds primarily kept for veterinary medicinal purposes is considered stress-free (Hashim et al., 2012) and eliminates the controversial and unnecessary suffering of the unborn calves.

As mentioned above, PCL has been approved for various biomedical applications. *In vivo* and *in vitro* biocompatibility studies have not revealed cytotoxicity (Woodruff and Hutmacher, 2010; Corrales et al., 2012). However, it is important to investigate the biocompatibility of PCL when applied in new experimental settings since the scaffold production techniques may influence its biocompatibility (Cipitria et al., 2011). Thus, in this work, we have investigated the biocompatibility of PCL granules, electrospun PCL 3D fibre meshes, and the 3D-printed PLA supporting material using *in vitro* cytotoxicity assay with L929 cells according to ISO standard 10993-5 with extracts collected according to ISO standard 10993-12.

In the present study, a modified electrospinning setup with a novel collector design was utilized to fabricate highly porous 3D PCL fibre meshes, mimicking the collagen fibres of the extracellular matrix in soft tissue and thus omitting the use of *e.g.* matrigel. We assessed cell proliferation in the 3D meshes after seeding different numbers of JIMT-1 or MCF-7 breast cancer cells, MCF-10A normal-like breast epithelial cells, or adult human dermal fibroblasts using medium supplemented with DHS. Confocal laser scanning microscopy and cryosectioning was used to assess the 3D ingrowth of the cells in the fibre meshes. Cell-cell and cell-fibre interaction were also investigated using scanning electron microscopy (SEM). The results from this study may speed up the development and optimization of future 3D tumour models as physiologically relevant systems that can contribute to the 3R principles to reduce the use of animals in tumour biology and therapeutic studies.

2. Materials and methods

2.1. Preparation of electrospun PCL fibre meshes

The highly porous unique fibre meshes were prepared in collaboration with Cellevate AB. Briefly, a polymeric solution of 15% PCL *w/v* (Sigma-Aldrich Sweden AB, Stockholm, Sweden) with an average molecular weight of 80 kDa was prepared by dissolving the PCL pellets in acetone (Sigma-Aldrich Sweden AB) under gentle stirring condition overnight at room temperature. The electrospinning process was performed horizontally with a syringe pump (Aladdin-1000, World Precision Instruments, Sarasota, FL, USA) set at a continuous flow rate of 2.0 mL/h^{-1}, a high voltage power supply (20 kV) (FuG Elektronik GmbH, Schechen, Germany), and a blunt needle tip with a distance of 20 cm to the stationary custom-made collector (Jakobsson et al., 2017). The electrospinning procedure was performed at room temperature with around 30–35% humidity. The randomly oriented fibre mesh for contact angle measurements was collected on a rotating collector (rotation speed 20 rpm) in the form of non-woven fibre mesh.

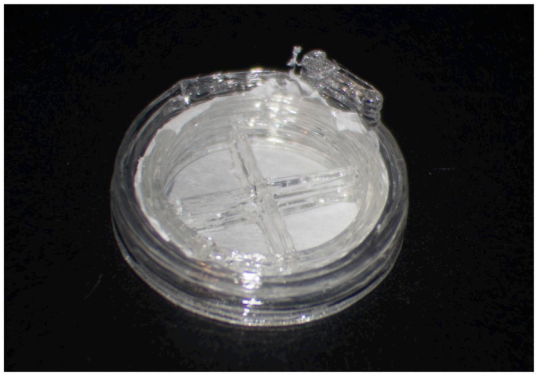

Fig. 1. Image of the 3D fibre unit consisting of the uncompressed PCL fibre mesh supported in lock-rings made of PLA. The fibre mesh that is very delicate is kept from bulging by a cross-shaped structure made of PLA. The diameter of the set-up is 10 mm and it is placed in a well of a hydrophobic 48-well plate before seeding of cells.

2.2. PCL fibre support units

In order to provide support for the non-compressed fibre network, 3D-printed polylactic acid (PLA) lock-rings were fabricated using a MakerBot Replicator 2 3D printer (Makerbot Industries, New York, NY, USA). Each fibre substrate was transferred from the tip of the collector and mounted in the lock-rings. The fibre mesh with diameter of 10 mm is kept from bulging by a 3D-printed cross-shaped structure made of PLA (Fig. 1).

2.3. Surface modification by plasma treatment and sterilization

PCL is intrinsically hydrophobic while the ECM microenvironment is hydrophilic. Thus, to obtain a hydrophilic substrate compatible with optimal cell attachment, the PCL fibres were modified by O_2 plasma treatment. A plasma-preen Ii-973 Tappan space saver microwave oven cleaner/etcher and a plasma-preen controller (Plasmatic Systems, Inc., North Brunswick, NJ, USA) were used for this purpose. O_2 plasma treatment was carried out for 15 s under 10 mbar pressure. The plasma-treated 3D fibre units were used within 1–2 days of treatment. Before cell addition, the 3D fibre units were immersed in 99.5% ethanol for 15 min and were then rinsed three times with sterile phosphate-buffered saline (PBS).

2.4. Contact angle measurements

Flat electrospun PCL fibre meshes were prepared in order to determine the contact angle, since it was not possible to perform the experiment on PCL fibre meshes in the lock-rings. The static water contact angle of PCL fibres was measured at room temperature, both before and after plasma treatment. Water droplets (6 µl) were applied at different random locations on untreated and plasma-treated fibre samples and images were taken with an EOS 600D Canon camera (Canon Inc., Tokyo, Japan) assembled on a Leica MZ6 Stereomicroscope (Leica Biosystems, Wetzlar, Germany). The water contact angles were determined using Java ImageJ software (http://imagej.nih.gov/ij/) and ImageJ contact angle plugin at least six times for each sample. No image editing was done prior to contact angle measurements.

2.5. Cell lines

The human breast cancer cell line JIMT-1 (ACC-589) was purchased from the German Collection of Microorganisms and Cell Cultures (Braunschweig, Germany). The human breast cancer cell line MCF-7 (HTB-22), the normal-like breast epithelial MCF-10A cell line (CRL-10317), and mouse L929 fibroblasts (CCL-1) were purchased from American Type Culture Collection (Manassas, USA). Human adult dermal fibroblasts were purchased from Sigma-Aldrich Sweden AB.

All the cell lines were cultured in Dulbecco's modified Eagle medium/Ham's F-12 supplemented with 5% heat-inactivated donor horse serum (Sigma-Aldrich Sweden AB), 10 µg/ml insulin (Sigma-Aldrich Sweden AB), 20 ng/ml epidermal growth factor (Lonza, USA), 0.25 µg/ml hydrocortisone (Sigma-Aldrich Sweden AB), 0.2 mM Na-pyruvate, 0.05 mg/ml transferrin (Sigma-Aldrich Sweden AB), 2 mM L-glutamine (VWR, Lund, Sweden), 1 mM non-essential amino acids (VWR), 100 µg/ml streptomycin (VWR), and 100 U/ml penicillin (VWR). In addition, the medium of the MCF-10A cells was supplemented with 50 ng/ml cholera toxin (Sigma-Aldrich Sweden AB). In addition, the medium of the MCF-7 cells was supplemented with 10 nM β-estradiol (Sigma-Aldrich Sweden AB). All cell lines were maintained in a humidified incubator containing 95% air and 5% CO_2 at 37 °C. The cells were passaged twice a week using Accutase (Sigma-Aldrich Sweden AB).

2.6. Seeding in 3D PCL fibre units

After detachment with Accutase® (Sigma-Aldrich Sweden AB), the number of cells was determined by counting in a hemocytometer. Cell suspensions containing a defined number of cells per ml were prepared (see Fig. 4). One ml was added to the 3D fibre units, which were placed in the wells of hydrophobic 48 well plates. The plates were kept in the CO_2 incubator at 37 °C for 1 week. The medium was replaced with 1 ml fresh medium after 72 h of incubation.

2.7. AlamarBlue® assay

On days 1–4 and day 7 after seeding, the AlamarBlue® assay (ThermoFisher Scientific, Waltham, MA, USA) was used to get an indirect estimate of cell number in the fibre mesh. AlamarBlue® is reduced at the level of oxygen in the electron transport chain and the read out is proportional to the cell number (Ahmed et al., 1994; Goegan et al., 1995; Nociari et al., 1998). AlamarBlue® reagent (100 µl) was added to the medium of the wells, the plate was covered with aluminium foil, which was then incubated for 4 h in the CO_2 incubator. Then 100 µl aliquots were removed for determination of reduced AlamarBlue® by measuring fluorescence at a wavelength of 590 nm after excitation at 540 using a SpectraMax® i3x multi-mode microplate reader (Molecular Devices, San Jose, CA, USA). The experiment was repeated at least three times for each seeding density with $n = 2$ in each experiment.

2.8. Fixation and staining of cultures

After the AlamarBlue® assay, the cultures with fixed in 3.7% formaldehyde in PBS for 15 min at 4 °C. Then the cultures were washed three times with PBS before blocking and permeabilization in 500 µl of blocking solution (1% dry milk and 1% Tween 20 in PBS) at room temperature for 1 h. Then the cells were stained with Alexa Fluor 488 phalloidin (ThermoFisher Scientific, A12379), diluted 1:100 in blocking buffer. The incubation of the cells continued for 2 h at room temperature. Then the samples were washed three times with PBS and incubated with 4′,6-diamidine-2′-phenylindole dihydrochloride (DAPI) (Sigma-Aldrich Sweden AB) (1 µg/ml PBS) for 1.5 min at room temperature. Thereafter, the 3D fibre units were mounted in Mowiol (Sigma-Aldrich Sweden AB) on glass cover slips and kept in darkness at 4 °C. The cells were imaged by epifluorescence and confocal microscopy.

2.9. Scanning electron microscopy

After 7 days of incubation, the 3D cultures were fixed in 3.7% paraformaldehyde for 30 min followed by washing 3 times with PBS. Thereafter the 3D cultures were subjected to dehydration in an hexamethyldisilane (HMDS) series (25%, 50%, 75%, and 100%, 15 min in each step) and then they were left to dry at room temperature overnight before mounting on aluminium stubs using adhesive carbon tape. The samples were then sputter-coated with a thin layer (12 nm) of gold using a Cressington 108auto sputter coater (Cressington Scientific Instruments Ltd.) for 55 s at 20 mA. The samples were viewed in a SEM (Model SU3500, Hitachi, Krefeld, Germany) and images were captured.

2.10. Confocal laser scanning microscopy

For visualization of cell distribution within 3D meshes, filamentous actin (F-actin) was labelled with Alexa Fluor 488 Phalloidin (ThermoFisher Scientific, A12379) and cell nuclei with DAPI. The cells were viewed in a Zeiss LSM 510 META confocal laser scanning microscope (Zeiss, Oberkochen, Germany) and images were taken with a 63×, 1.4 NA oil immersion objective lens.

For acquisition of z-stack images of the 3D cultures, the stained samples were immersed in a 2.2′-thiodiethanol (TDE) (Sigma-Aldrich Sweden AB) dilution series (10%, 25%, 50%, and 97%, 10 min in each step). Then, samples were mounted on cover slips with 97% TDE in PBS. *Z*-stack images were taken with 25×, 1.2 NA oil immersion objective lens and images were analysed with ZEN software (Zeiss).

2.11. Biocompatibility evaluation

2.11.1. Polymer extraction

In order to analyse the biocompatibility of the 3D units, extracts of PCL granules, the PCL fibre mesh, and PLA lock ring material were prepared according to ISO standard 10993-12. The polymers were added to sterile pre-weighed borosilicate glass flasks and then the flasks were weighed again to obtain the weight of the polymer. The polymers were washed with 70% ethanol, rinsed with water, and dried. Sterile Millipore water (1 ml/0.2 g) was then added, the lid tightened and the flasks kept at 37 °C for 72 h. The extraction solution was sterile-filtered before testing in an MTT dose response assay.

2.11.2. MTT assay

The MTT assay was used to evaluate the cytotoxicity of polymer extracts in L929 cells according to ISO standard 10993-5. Different concentrations of extract in 2× concentrated L929 medium were prepared (1:2 (yields 0.1 g/ml), 1:4 (yields 0.05 g/ml), 1:8 (yields 0.025 g/ml), 1:16 (yields 0.0065 g/ml), 1:32 (yields 0.00325 g/ml), and 1:64 (yields 0.00163 g/ml). L929 cells were seeded in complete cell culture medium in 96-well plates at a density of 5000 cells in 150 µl medium per well and incubated at 37 °C overnight to allow attachment. Thereafter, the medium was removed and 150 µl of medium with the respective concentrations was added. As positive controls, DMSO was added to an equal amount of 2× medium to obtain three different concentrations; 5%, 2%, and 1%. As negative control, distilled water was added to an equal amount of 2× medium. The 96-well plates were incubated for 72 h followed by indirect evaluation of the cell number using the MTT (3-(4, 5- dimethylthiazol-2-yl)-2,5-diphenyltetrazolium bromide) assay. To each well, 20 µl MTT solution (5 mg/ml PBS) was added and the 96-well plates were incubated in the CO_2 incubator for 1 h protected from light by covering with aluminium foil. The MTT containing medium was removed and formazan crystals formed in the live cells by reduction of MTT in the mitochondrial electron transport chain were dissolved by adding 100 µl DMSO and the plate was

incubated for 10 min at room temperature. The formed formazan crystals yielding a blue purple colour upon dissolution in DMSO is assumed to be proportional to cell number. The optical density of each well was analysed at 540 nm using a microplate reader (ThermoFisher Scientific). The experiment was repeated at least three times with new polymer extracts each time.

2.12. Cryosectioning

After fixation of 7 days of cultures and staining, the 3D meshes freed of the PLA lock rings were embedded in tissue freezing medium Optimal Cutting Temperature (Histolab, Askim, Sweden) for 30 min at −20 °C. Sectioning was performed using a Leica CM1950 Cryostat (Leica Biosystems) at −20 °C. The sample was initially trimmed with a razor blade and then sections of 30 µm thickness were collected on Polysine™ glass slides (Menzel GmbH & Co., Berlin, Germany). The samples were washed three times with PBS to remove the freezing medium. They were mounted with Mowiol and stored at −20 °C until microscopic visualization.

3. Results

3.1. Contact angle measurement

Intrinsically PCL is hydrophobic and since optimal cell attachment is dependent on a hydrophilic surface, we used plasma treatment to insert oxygen into the PCL fibres. However, O_2 plasma treatment is a rather harsh procedure and the fibres can become distorted. Comparing the images of Figs. 2 A-B and D-E show that plasma treatment for 15 s under 10 mbar pressure does not affect the morphology of the fibres. Longer treatment times resulted in melting of the fibres (not shown).

Fig. 2C and 2F show the water contact angles of untreated PCL fibres and plasma-treated PCL fibres with contact angle measurements of 113° and 43°, respectively. Thus, plasma treatment for 15 s does not affect the fibre structure mesh and the PCL fibres become hydrophilic. Thus, for all experiments, the 3D fibre units were subjected to plasma treatment before seeding of cells.

3.2. Biocompatibility of electrospun PCL fibre units

In order to ensure that the 3D fibre unit is not toxic, we performed a biocompatibility test of extracts of PCL granules, PCL fibres, and PLA support material according to ISO standard 10,993–12. Different concentrations of extracts were tested using the mouse fibroblast L929 cell line treated for 72 h and then evaluated with an MTT colorimetric assay. Fig. 3 shows that none of the extracts displayed toxicity.

3.3. Evaluation of cell proliferation of cells seeded in 3D fibre units

The AlamarBlue® assay was used as an indirect measure to determine if there was a change in cell number during 1 week after seeding cells. An increase in AlamarBlue® reduction indicates an increase in cell number. Human breast cancer JIMT-1 and MCF-7 cells, normal-like human breast epithelial MCF-10A cells, and human adult dermal fibroblasts were seeded at two different densities (a lower and a higher, Fig. 4) to get an understanding of how initial seeding density affects the behaviour of the cells. These seeding densities were partly based on the cell cycle time of the respective cell lines as well as on the seeding density used when culturing them in 2D monolayer. In general, there was an increase in AlamarBlue® reduction during day 3 to day 7 indicating an increase in cell number after a 48-h lag period (day 1 and day 2). However, the lag period was somewhat shorter when the cells were seeded at a higher density. Independent on the initial seeding density, the AlamarBlue® reduction was similar on day 7 after seeding. Based on these data, we decided to seed the cells at the lower density for each cell line in further experiments.

3.4. Morphological evaluation of cells seeded in 3D fibre units

We used SEM to investigate the morphology of cells on or close to the surface area of the 3D meshes and confocal microscopy to investigate how deep the cells grow into the meshes. The SEM microscopy was performed on day 7 cultures and the images only show cells on the surface of the fibre mesh (Fig. 5). The MCF-7 cells are found growing in tight clusters of different sizes which probably reflects their epithelial features (Fig. 5A) (Takeichi, 1995). The image of the JIMT-1 cells shows a diverse morphology, with both round and flat cells, the latter seemingly attached to fibres. The MCF-10A and human dermal fibroblasts have a spread-out flat morphology and tend to adhere to multiple fibre

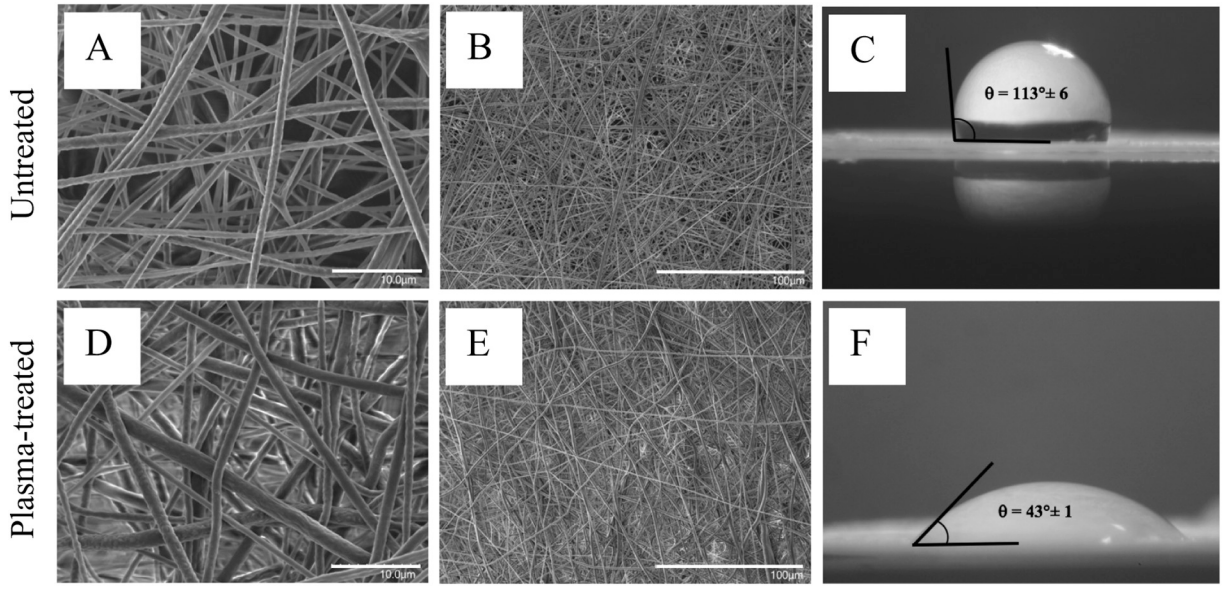

Fig. 2. Scanning electron images of electrospun PCL fibre meshes and contact angle measurements before (A, B, and C) and after O_2 plasma treatment (D, E, and F). The water contact angle values are presented as mean ± SEM (n = 6). Scale bars indicate 10 (images to the left) and 100 µm (images in the middle).

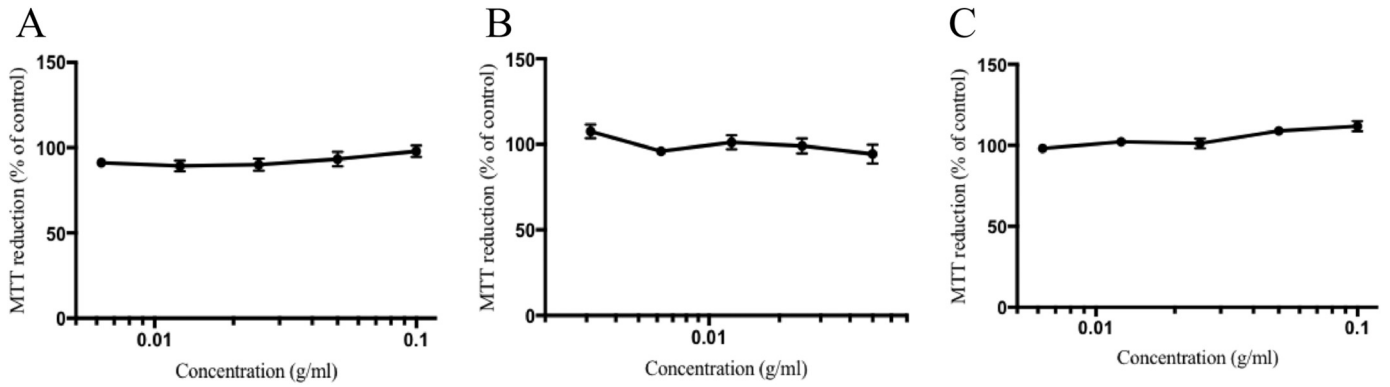

Fig. 3. Biocompatibility of extracts of (A) PCL granules, (B) PCL fibres, and (C) PLA used in lock rings evaluated in L929 cells using dose response assays with MTT reduction as readout. The cells were seeded in 96-well plates and 24 h later, the cells were subjected to medium with different concentrations of extract. After 72 h of treatment, an MTT assay was used for evaluation of toxicity. The values are based on the mean ± SEM of three independent experiments with 6 wells per concentration in each experiment.

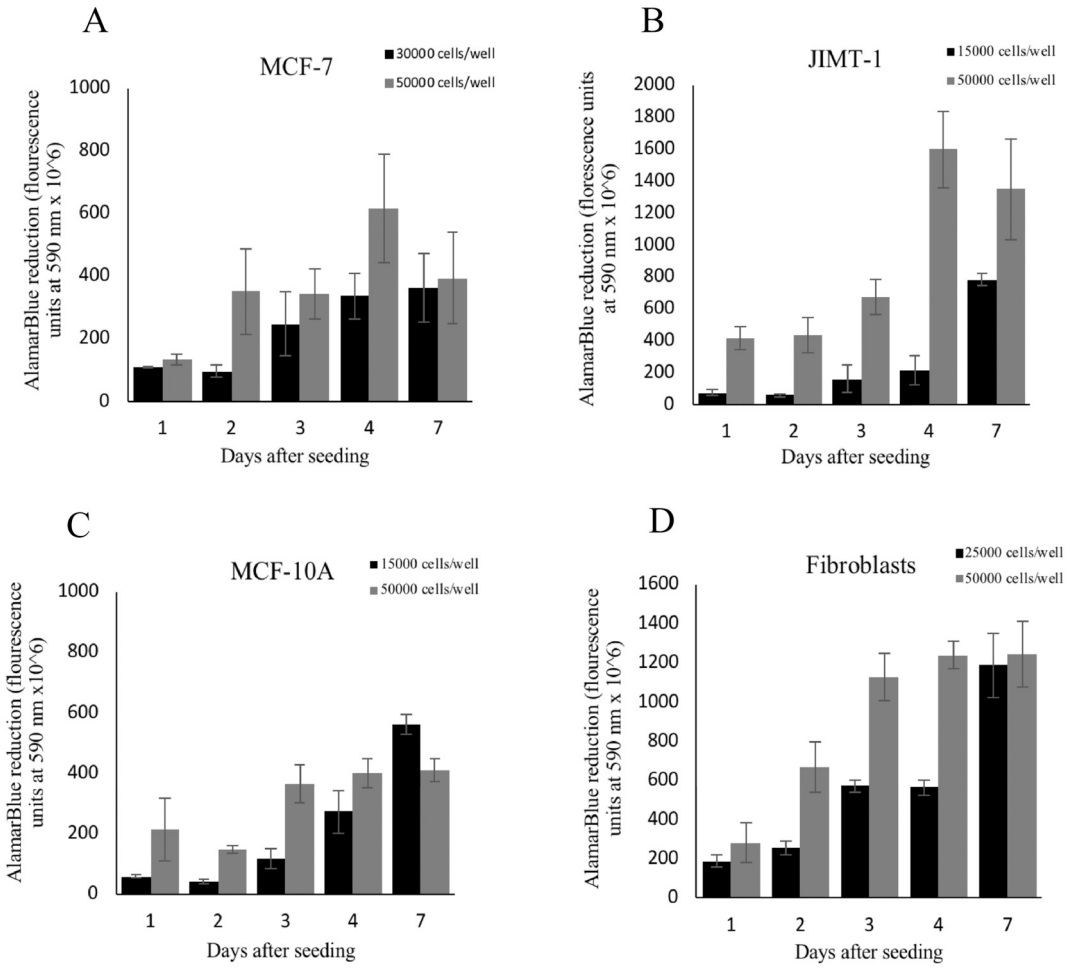

Fig. 4. AlamarBlue® reduction as an indirect estimation of cell number of MCF-7 (A), JIMT-1 (B), MCF-10A (C), and human fibroblasts (D) seeded at two different densities in 3D PCL fibre meshes. Cells were seeded in 3D fibre units on day 0. At 1–4 and 7 days after seeding, AlamarBlue ®was added to the medium and after 4 h of incubation, the reduction of AlamarBlue® was determined in a spectrophotofluorometer. Each column shows the mean ± SE of three independent experiments with three 3D fibre units in each.

(Fig. 5C and D, respectively).

Fig. 6 shows confocal laser scanning microscopy images of cells found on the surface of the 3D fibre mesh after 7 days of incubation (Fig. 6). All the cell lines were stained to visualize the actin cytoskeleton and cell nuclei to analyse the morphology of cells. The cells show similar morphology as in the SEM images (compare with Fig. 5).

3.5. Cell infiltration into 3D fibre meshes

Confocal microscopy z-stack imaging shows infiltration of cells deep into the 3D fibre meshes 7 days after seeding the cells (Fig. 7). Thus, the PCL fibre mesh, which has an average pore size of 50 μm^2, provides adequate spacing and porosity permitting cell infiltration (Jakobsson

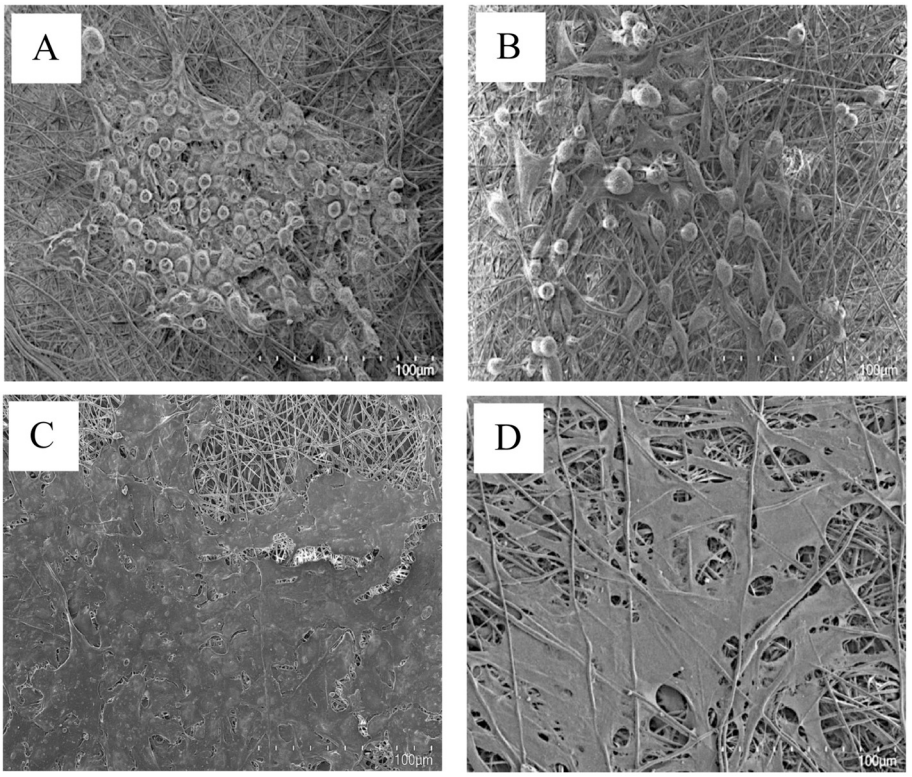

Fig. 5. Scanning electron microscopy images of cells seeded in 3D PCL fibre meshes after 1 week of incubation. (A) MCF-7 cells, (B) JIMT-1 cells, (C) MCF-10A cells, and, (D) human adult dermal fibroblasts on the surface of 3D PCL fibre meshes. Scale bars indicate 100 µm.

et al., 2017). The breast cancer cells form small tight spheroids at different depths of the mesh while fibroblasts are spread-out in the mesh. The MCF-10A cultures show both clusters of cells and a spread-out morphology of the cells in the mesh.

The 3D cultures were also cryosectioned to further confirm cell infiltration into the fibre network (Fig. 8). The combined fluorescence and differential interference contrast microscopy images show the fibres with infiltrating cells (Fig. 8). Haematoxylin- and eosin-stained

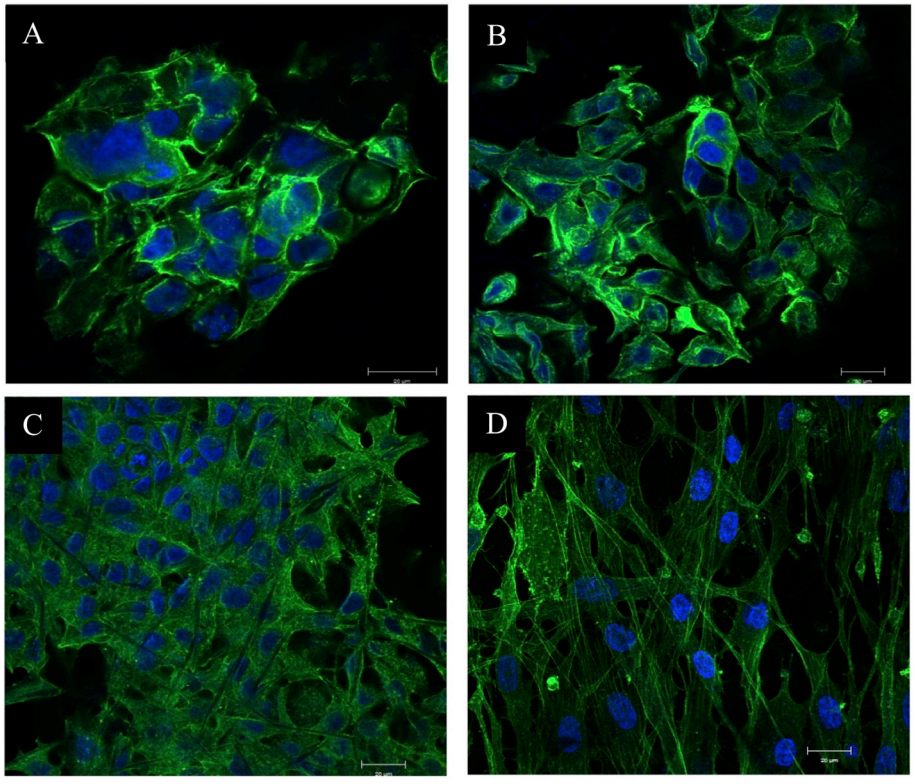

Fig. 6. Morphological comparison using confocal microscopy of different cells seeded in 3D PCL fibre meshes after 1 week of incubation. Confocal scanning microscopy images of (A) MCF-7 cells, (B) JIMT-1 cells, (C) MCF-10A cells, and (D) human adult dermal fibroblasts on the surface of 3D PCL fibre meshes. The cells were stained with Alexa 488-phalloidin (green) to visualize actin cytoskeleton and DAPI (blue) to visualize nuclei. Scale bars indicate 20 µm. Compare with Fig. 5.

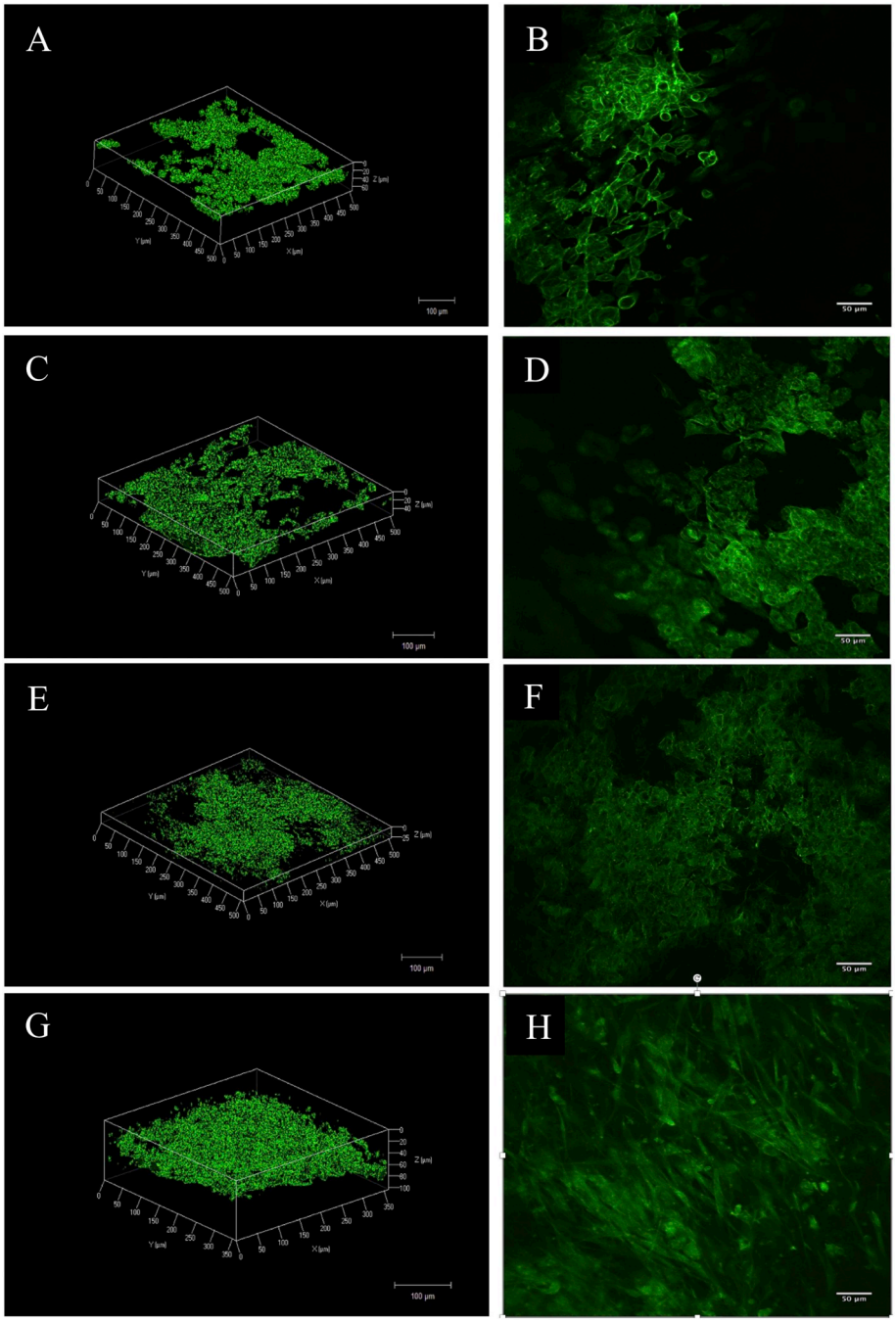

Fig. 7. Infiltration of human breast cancer cells and human normal cells in the 3D PCL fibre meshes after 1 week of incubation. Confocal microscopy *Z*-stack imaging of (A, B) MCF-7 cells, (C, D) JIMT-1 cells, (E, F) MCF-10A cells, and (G, H) human adult dermal fibroblasts. A, C, E, and G: 3D images. B, D, F, and H: single confocal plane. The cells were stained with Alexa 488-phalloidin (green) to visualize the actin cytoskeleton (left). All images were taken with a 25× oil immersion objective lens. Scale bars indicate 100 (A, C, E, and G) and 50 (B, D, F, and H) μm.

cryosectioned samples showing a similar growth pattern are found in the supplementary information (Fig. S2). The cryosectioning has exerted some tear force on the meshes as is shown by the sprouting fibres. All of the cryosectioned images show infiltration of cells into a fibre mesh depth of approximately 100 μm. A certain degree of compression of the fibre mesh is expected by all the procedures they encounter from cell seeding, fixation, washing, staining, and embedding *etc.*

4. Discussion

In order to increase the performance of *in vitro* experiments, cells should be provided with a 3D substrate that mimics the complex ECM found in tissue. A vital supportive component of the ECM is the fibrous collagen which composes up to the 30% of the body protein. Thus, collagen is used to form porous 3D fibre networks, which indeed support normal cellular activities *i.e.* more resembling *in vivo* behaviour than 2D cell culturing does (Chevallay and Herbage, 2000; Lv et al., 2016). Another commonly used product for 3D cell culturing is matrigel which also contains a high percentage of collagen in addition to *e.g.* laminin. In general, collagen used in cell culturing is of bovine, murine, or rat origin and matrigel is derived from the EHS mouse sarcoma. In an attempt to avoid animal-derived collagen but yet have a collagen-like fibrous structure, we have used highly porous 3D PCL fibre meshes fabricated using a unique electrospinning set up (Jakobsson et al.,

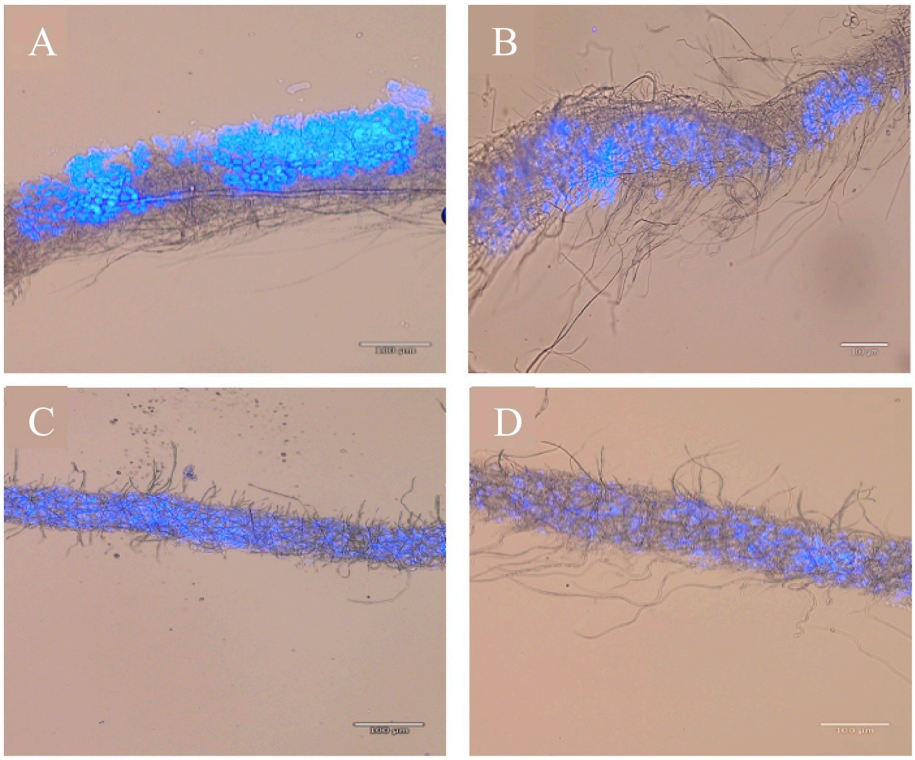

Fig. 8. Cryosectioned samples show infiltration of human breast cancer and human normal cells into the 3D PCL fibre mesh after 1 week of incubation. Combined differential interference contrast and fluorescence microscopy images of cryosectioned 3D PCL fibre meshes of (A) MCF-7 cells, (B) JIMT-1 cells, (C) MCF-10A cells, and (D) human adult dermal fibroblasts. The cell nuclei were stained with DAPI (blue) for visualization. The meshes are to some degree compressed and some fibres are pulled out due to the cryosectioning procedure. Scale bars indicate 100 µm.

2017). The uncompressed randomly-oriented organization of electrospun fibres represent the topography of natural stromal collagen fibres. PCL has been used extensively in electrospinning (Azimi et al., 2014), however, our 3D fibre mesh is unique regarding its synthesis enabling the formation of the highly uncompressed fibre structure in contrast to standard electrospinning using PCL, which results in a denser fibre structure compared to the fibre mesh used here.

The most commonly used plastic in cell culturing is polystyrene, which in its native form is highly hydrophobic and does not permit cell attachment. Companies producing cell culture plastics use different methodologies to introduce oxygen containing groups into the polystyrene surface materials *e.g.* plasma irradiation, chemical vapor deposition, ultraviolet irradiation, and etching (Yoshihisa et al., 2013), which renders the surface hydrophilic. Similarly, to polystyrene, PCL is an intrinsically hydrophobic polyester and we and others have indeed observed decreased cell attachment to native PCL (Jacobs et al., 2011). Based on the fact that a hydrophilic surface is required to obtain optimal cell attachment, we used O_2 plasma treatment to obtain hydrophilic PCL fibre meshes. Water contact angle measurements of untreated PCL meshes proved their hydrophobic nature while water contact angle measurements of O_2 plasma-treated PCL showed that the treatment indeed resulted in hydrophilic substrates. Martins et al. (2009) showed that the most favourable contact angle values for cell adhesion lie in the range between 20° and 70° and thus, we conclude that the contact angle of 43° of O_2 plasma-treated PCL is most suitable and the treatment left no detectable morphological changes on the topography of the fibres.

To ascertain that the materials used in this study does not leak any molecules *e.g.* monomers that could affect the cells, we performed a biocompatibility study of the individual components of the 3D culture unit. All materials have previously been shown to be non-toxic and biofriendly, but the effect of the 3D culture unit's fabricating techniques *i.e.* electrospinning and 3D-printing could perhaps affect the material properties. To address this issue, extracts were collected according to ISO standard 10993-12 using water as extraction medium. In order to obtain the solutions, extraction was conducted at 37 °C, simulating body temperature (incubator temperature), for 72 h. Cytotoxicity was then tested using an MTT assay on L929 cells according to ISO standard 10993-5. The test showed no toxicity of any of the components (PCL granules, PCL fibres, or PLA support) used in the 3D fibre mesh units and thus confirmed the previous observed biocompatibility of the polymer materials. Furthermore, the result show that the materials are not affected due to the techniques used here.

As no toxicity was found, we proceeded with seeding cells from two human non-malignant cell lines, MCF-10A and human adult dermal adult fibroblasts, and two malignant breast cancer cell lines, MCF-7 and JIMT-1, into the 3D fibre meshes. Before these experiments, however, we adapted the protocols for these cell lines to thrive in medium supplemented with DHS instead of FBS to remove the latter animal ethically questionable product. In the initial experiments, we decided to seed cells at two different densities, one lower and one higher, to get an understanding of their growth behaviour in 3D fibre meshes. To the best of our knowledge, we have not found such investigations comparing different seeding densities in 3D PCL-based cultures. We used the AlamarBlue® assay to get an indirect estimation of cell number. The AlamarBlue® assay is a non-destructive assay used for cytotoxicity, biocompatibility, viability, as well as proliferation studies, that has been applied for very long in 2D cultures and also lately in 3D cell cultures (van Gaalen et al., 2010). Our data show that the growth pattern varies with seeding density for all four cell lines, the lower density resulting in a longer lag phase while the cells reached a plateau phase in 7 days, while seeding at the high density resulted in shorter lag phase with plateau phase reached 3 days after cell seeding. Similar conclusions have been drawn for cells seeded in other 3D structures than fibrous PCL scaffolds (Zhou et al., 2011; Dar et al., 2002; Yassin et al., 2015). Moreover, Neuhuber et al. (2008) found that low initial seeding density of human mesenchymal stem cells enhanced the yield and expansion of these cells. Due to the proliferation pattern in the 3D fibre meshes, we decided to use the lower density for further characterization studies.

Rapid infiltration is a crucial factor for 3D integration of cells into the depth of fibre networks and hence formation of 3D cellular structures *in vitro* (Szot et al., 2009; Wu and Hong, 2016). Both confocal microscopic analysis and as well as microscopic analysis of cryosections

showed that the cells indeed penetrate into the fibre mesh at different depths. The fibre mesh thickness before seeding cells is approximately 250 µm. However, the fibrous net is delicate and can easily be compressed and thus, it is most probable that the different procedures used during handling of the 3D cultures results in compression of the network. The cryosectioning clearly resulted in partial rupture of fibres. However, taken together, the data show good cell penetration of all four cell lines but interestingly the growth pattern is different between malignant and non-malignant cells. The malignant cells grow as small spheroids, interacting partially with the fibres while fibroblasts and the MCF-10A cells instead spread out between fibres and along the fibres forming elongated and more sheet like structures. Aggregation of cells on fibrous meshes are closely associated with incubation time and initial seeding concentration of cells, as the increase in time and number of cells lead to the formation of bigger and higher number of spheroids which has also been observed by others (Girard et al., 2013). Cell infiltration into 3D PCL fibre networks has previously been demonstrated for human bone marrow cells (Brennan et al., 2015), and this is clearly also the case for the here tested cell types.

5. Conclusion

Scaffold-based 3D culture models have provided a great potential to study the phenotype of normal and malignant cells in a microenvironment with physiological resemblance to organ structure and function *in vivo*. Cells display different biological properties when cultured in 3D fibrous meshes due to complex mechanical and biochemical 3D cues which are absent in 2D cell cultures (Sun et al., 2006). Herein, a modified electrospinning method with a custom-made collector was utilized to fabricate highly porous 3D PCL nanofibre meshes that were subjected to O_2 plasma treatment to become hydrophilic. We have successfully demonstrated that different cell types, malignant as well as normal thrive in the 3D fibre unit. We are presently exploring this model for co-culturing of cancer cells and different types of stromal cells. We anticipate this model can be used to create a 3D tumour *ex vivo* platform that can be used for screening of therapeutic compounds, which will reduce the number of animals in cancer research.

Acknowledgements

The authors are grateful to the Forska Utan Djurförsök, Carolina Le Prince with the “Kalenderflickorna”, NanoLund, and Crafoord Foundation for funding of this work. We thank Helena Fritz for excellent technical assistance with cell seeding.

Disclosure

We hereby declare the following competing financial interest: the co-author, Fredrik Johansson, is a co-founder, shareholder, and consultant, of the Cellevate AB company in Sweden.

Appendix A. Supplementary data

Supplementary data to this article can be found online at https://doi.org/10.1016/j.tiv.2019.04.022.

References

Ahmed, S.A., Gogal Jr., R.M., Walsh, J.E., 1994. A new rapid and simple non-radioactive assay to monitor and determine the proliferation of lymphocytes: an alternative to H3-thymidine incorporation assay. J. lmmunol. Methods 170, 211–224. https://doi.org/10.1016/0022-1759(94)90396-4.

Anisimov, V.N., Ukraintseva, S.V., Yashin, A.I., 2005. Cancer in rodents: does it tell us about cancer in humans? Nat. Rev. Cancer 5, 807. https://doi.org/10.1038/nrc1715.

Azimi, B., Nourpanah, P., Rabiee, M., et al., 2014. Poly (ϵ-caprolactone) Fiber: an overview. J. Eng Fibers Fabr. 9 (3). https://doi.org/10.1177/155892501400900309.

Bielecka, Z.F., Maliszewska-Olejniczak, K., Safir, I.J., et al., 2017. Three-dimensional cell culture model utilization in cancer stem cell research. Biol. Rev. 92, 1505–1520. https://doi.org/10.1111/brv.12293.

Brennan, M.A., Renaud, A., Gamblin, A.L., et al., 2015. 3D cell culture and osteogenic differentiation of human bone marrow stromal cells plated onto jet-sprayed or electrospun micro-fiber scaffolds. Biomed. Mater. 10, 045019. https://doi.org/10.1088/1748-6041/10/4/045019.

Chevallay, B., Herbage, D., 2000. Collagen-based biomaterials as 3D scaffold for cell cultures: applications for tissue engineering and gene therapy. Med. Biol. Eng. Comput. 38, 211–218. https://doi.org/10.1007/BF02344779.

Cipitria, A., Skelton, A., Dargaville, T.R., et al., 2011. Design, fabrication and characterization of PCL electrospun scaffolds-a review. J. Mater. Chem. 21, 9419–9453. https://doi.org/10.1039/c0jm04502k.

Corrales, T., Larraza, I., Catalina, F., et al., 2012. In vitro biocompatibility and antimicrobial activity of poly(ε-caprolactone)/montmorillonite nanocomposites. Biomacromolecules 13, 4247–4256. https://doi.org/10.1021/bm301537g.

Dar, A., Shachar, M., Leor, J., Cohen, S., 2002. Optimization of cardiac cell seeding and distribution in 3D porous alginate scaffolds. Biotechnol. Bioeng. 80, 305–312. https://doi.org/10.1002/bit.10372.

Feng, S., Duan, X., Lo, P.K., et al., 2013. Expansion of breast cancer stem cells with fibrous scaffolds. Integr Bio Royal Soc. Chem. 5, 768–777. https://doi.org/10.1039/C3IB20255K.

Foroni, L., Vasuri, F., Valente, S., et al., 2013. The role of 3D microenvironmental organization in MCF-7 epithelial-mesenchymal transition after 7 culture days. Exp. Cell Res. 319, 1515–1522. https://doi.org/10.1016/j.yexcr.2013.03.035.

Frenot, A., Chronakis, I.S., 2003. Polymer nanofibers assembled by electrospinning. Curr. Opin. Colloid Interface Sci. 8, 64–75. https://doi.org/10.1016/S1359-0294(03)00004-9.

Girard, Y.K., Wang, C., Ravi, S., et al., 2013. A 3D fibrous scaffold inducing tumoroids: a platform for anticancer drug development. PLoS One 8. https://doi.org/10.1371/journal.pone.0075345.

Goegan, P., Johnson, G., Vincent, R., 1995. Effects of serum protein and colloid on the AlamarBlue assay in cell cultures. Toxicol. in Vitro 9, 257–266. https://doi.org/10.1016/0887-2333(95)00004-R.

Hashim, Y.Z.H.-Y., Mel, M., Salleh, H.M.A., et al., 2012. Serum in mammalian cell culture: weighing the challenges of bioprocessing, ethics and animal welfare. Adv. Nat. Appl. Sci. 6, 596–600,. http://www.aensiweb.com/old/anas/2012/596-600.pdf.

Jacobs, T., Morent, R., De, G.N., et al., 2011. Visualization of the penetration depth of plasma in three-dimensional porous PCL scaffolds. IEEE Trans. Plasma Sci. 39, 2792–2793. https://doi.org/10.1109/TPS.2011.2128894.

Jakobsson, A., Ottosson, M., Zalis, M.C., et al., 2017. Three-dimensional functional human neuronal networks in uncompressed low-density electrospun fiber scaffolds. Nanomedicine 13, 1563–1573. https://doi.org/10.1016/j.nano.2016.12.023.

Kim, J.B., 2005. Three-dimensional tissue culture models in cancer biology. Semin. Cancer Biol. 15, 365–377. https://doi.org/10.1016/j.semcancer.2005.05.002.

Kim, T.E., Kim, C.G., Kim, J.S., et al., 2016. Three-dimensional culture and interaction of cancer cells and dendritic cells in an electrospun nano-submicron hybrid fibrous scaffold. Int. J. Nanomedicine 11, 823–835. https://doi.org/10.2147/IJN.S101846.

Knight, E., Przyborski, S., 2015. Advances in 3D cell culture technologies enabling tissue-like structures to be created in vitro. J. Anat. 227, 746–756. https://doi.org/10.1111/joa.12257.

Lv, D., Yu, S., Ping, Y., et al., 2016. A three-dimensional collagen scaffold cell culture system for screening anti-glioma therapeutics. Oncotarget 7, 56904–56914. https://doi.org/10.18632/oncotarget.10885.

Martins, A., Pinho, E.D., Faria, S., et al., 2009. Surface modification of electrospun polycaprolactone nanofiber meshes by plasma treatment to enhance biological performance. Small 5, 1195–1206. https://doi.org/10.1002/smll.200801648.

Neuhuber, B., Swanger, S.A., Howard, L., et al., 2008. Effects of plating density and culture time on bone marrow stromal cell characteristics. Exp. Hematol. 36, 1176–1185. https://doi.org/10.1089/ten.tea.2011.0048.

Nociari, M.M., Shalev, A., Benias, P., et al., 1998. A novel one-step, highly sensitive fluorometric assay to evaluate cell-mediated cytotoxicity. *J. Immunol. Methods*. **213**, 157–167. https://doi.org/10.1016/S0022-1759(98)00028-3.

Nyga, A., Loizidou, M., Cheema, U., 2011. 3D tumour models: novel in vitro approaches to cancer studies. J. Cell Comm. Signal. 5, 239–248. https://doi.org/10.1007/s12079-011-0132-4.

Rangarajan, A., Weinberg, R.A., 2003. Opinion: comparative biology of mouse versus human cells: modelling human cancer in mice. Nat. Rev. Cancer 3, 952–959. https://doi.org/10.1038/nrc1235.

Rangarajan, A., Hong, S.J., Gifford, A., Weinberg, R.A., 2004. Species- and cell type-specific requirements for cellular transformation. Cancer Cell 24, 394–398. https://doi.org/10.1016/j.ccr.2004.07.009.

Rijal, G., Li, W., 2016. 3D scaffolds in breast cancer research. Biomaterials 81, 135–156. https://doi.org/10.1016/j.biomaterials.2015.12.016.

Szot, C.S., Buchanan, C.F., Gatenholm, P., et al., 2009. Investigation of cancer cell behavior on nanofibrous scaffolds. Mater. Sci. Eng. C31, 37–42. https://doi.org/10.1016/j.msec.2009.12.005.

Sun, T., Jackson, S., Haycock, J.W., 2006. Culture of skin cells in 3D rather than 2D improves their ability to survive exposure to cytotoxic agents. *J. Biotechnol*. 122, 372–381. https://doi.org/10.1016/j.jbiotec.2005.12.021.

Szot, C.S., Buchanan, C.F., Freeman, J.W., Rylander, M.N., 2011. 3D in vitro bioengineered tumors based on collagen I hydrogels. Biomaterials 32, 7905–7912. https://doi.org/10.1016/j.biomaterials.2011.07.001.

Takeichi, M., 1995. Morphogenetic roles of classic cadherins. Curr. Opin. Cell Biol. 7, 619–627. https://doi.org/10.1016/0955-0674(95)80102-2.

Ulery, B.D., Nair, L.S., Laurencin, C.T., 2011. Biomedical applications of biodegradable polymers. J. Polym. Sci. B Polym. Phys. 49, 832–864. https://doi.org/10.1002/polb.22259.

Van der Valk, J., Mellor, D., Brands, R., et al., 2004. The humane collection of fetal bovine serum and possibilities for serum-free cell and tissue culture. Toxicol. in Vitro 18, 1–12. https://doi.org/10.1016/j.tiv.2003.08.009.

Van Gaalen, S.M., de Bruijn, J.D., Wilson, C.E., et al., 2010. Relating cell proliferation to in vivo bone formation in porous Ca/P scaffolds. J. Biomed. Mater. Res. 92, 303–310. https://doi.org/10.1002/jbm.a.32380.

Woodruff, M.A., Hutmacher, D.W., 2010. The return of a forgotten polymer—Polycaprolactone in the 21st century. Prog. Polym. Sci. 35, 1217–1256. https://doi.org/10.1016/j.progpolymsci.2010.04.002.

Wu, J., Hong, Y., 2016. Enhancing cell infiltration of electrospun fibrous scaffolds in tissue regeneration. Bioact. Mater. 1, 56–64. https://doi.org/10.1016/j.bioactmat.2016.07.001.

Yassin, M.A., Leknes, K.N., Pedersen, T.O., et al., 2015. Cell seeding density is a critical determinant for copolymer scaffolds-induced bone regeneration: copolymer scaffolds induced bone regeneration. J. Biomed. Mater. Res. A 103, 3649–3658. https://doi.org/10.1002/jbm.a.35505.

Yoshihisa, K., Yoshimura, A., Shibamori, Y., et al., 2013. Hydrophilic modification of plastic surface by using microwave plasma irradiation. IHI Eng. Rev. 46, 29–33. https://www.ihi.co.jp/var/ezwebin_site/storage/original/application/c73877fc235ab48d94af7b4563915734.pdf.

Zhou, H., Weir, M.D., Xu, H.H.K., 2011. Effect of cell seeding density on proliferation and osteodifferentiation of umbilical cord stem cells on calcium phosphate cement-fiber scaffold. Tissue Eng. 17, 2603–2613. https://doi.org/10.1089/ten.tea.2011.0048.